

## MICROCLIMATE EFFECTS ON BUILDING ENERGY USE: A METHODOLOGICAL APPROACH

J. Allegrini<sup>1</sup>, V. Dorer<sup>1</sup>, D. Derome<sup>1</sup>, J. Carmeliet<sup>1,2</sup>

<sup>1</sup>Laboratory for Multiscale Studies in Building Physics, Swiss Federal Laboratories for Materials Science and Technology (Empa), Dübendorf, Switzerland

<sup>2</sup>Chair of Building Physics, Swiss Federal Institute of Technology ETHZ, Zurich, Switzerland

Email: [jonas.allegrini@empa.ch](mailto:jonas.allegrini@empa.ch), [viktor.dorer@empa.ch](mailto:viktor.dorer@empa.ch), [dominique.derome@empa.ch](mailto:dominique.derome@empa.ch), [carmeliet@arch.ethz.ch](mailto:carmeliet@arch.ethz.ch)

### ABSTRACT

The urban heat island effect affects the energy use for cooling in an urban environment, as well as human comfort and health. Water evaporation from moist surfaces could potentially reduce the local temperature in urban areas, a process known as evaporative cooling. An important part of the heat exchange between buildings and the ambient surrounding is due to convective and radiative heat flows. The impact of these heat flows on energy consumption for cooling is much more important in urban areas compared to rural areas.

### INTRODUCTION

A major part of the final energy consumption in our nowadays society is due to buildings and cities. For the future, we have to find new urban energy concepts based on the integration of renewable energy supply, conversion, storage, distribution and management on neighbourhood or urban scale, where buildings will become interconnected, harvesting, exchanging and storing energy. The objective might be that local neighbourhoods become energy self-regulating, minimizing the additional supply from national or international energy systems. This challenging new concept has the potential to substantially decentralize the energy sector. The energy demand of neighbourhoods depends not only on their building energy systems, but also on the microclimate created around the buildings, which can differ substantially for rural, suburban and urban areas. Even for buildings in an urban context, common practice in detailed building energy simulation (BES) still relies on stand-alone building configurations, not accounting for the influence of neighbouring buildings, except perhaps for shading. However, the urban climate and microclimate can strongly affect the building energy demand. Thus, BES has to be coupled with an urban microclimate model.

We propose a methodology where the complex aspects of the urban microclimate are taken into account in order to properly estimate the environmental loading on buildings and, in counterpart, their energy behaviour. We present two examples. First, a coupled model is used to study the effect of evaporative cooling on the temperature

conditions in an urban street canyon. The model couples three sub-models: (i) a Computational Fluid Dynamics (CFD) model, which solves heat and vapour transfer in the air, (ii) a Building Envelope Heat and Moisture (BE-HAM) transport model which solves heat and moisture transfer within the porous building walls and (iii) a radiation model (RAD) which determines the radiative heat exchange between the surfaces. The effect of evaporation on the reduction of the surface and air temperatures and on comfort in a street canyon is analysed. Second, a study aims at quantifying the influence of the urban radiation balance, the urban heat island effect and urban convective heat transfer coefficients (CHTC) on the space cooling demands. CHTC correlations were determined using computational fluid dynamics (CFD) for different geometries. Buoyancy was accounted for by considering differences between building surface and surrounding air temperature. It was found that the building geometry has a large impact on the CHTC correlations and that the effect of buoyancy cannot be neglected when wind speeds are low. These CHTC correlations were used for Building Energy Simulation (BES) predictions of the space cooling demand. For accurate predictions of the space cooling demand, adequate CHTC correlations have to be used adjusted to the actual building configuration.

Before the two examples, our main tool, computational fluid dynamics (CFD) used to predict wind flow in urban areas is validated using wind tunnel data. Velocity, turbulent kinetic energy and temperature profiles from CFD are compared with the measured flow fields (measured with particle image velocimetry) for specific urban geometries. Isothermal cases as well as cases with heated surfaces were considered. The results show that CFD can predict the general flow structures and the influence of buoyancy. The detailed flow field inside the street canyon is strongly dependent on the flow structure within the shear layer at the top of the street canyon. Therefore to get accurate results for the flow profiles inside the street canyon and also for predicting the exchange rate between the street canyon and the flow above the canopy, the flow within the shear layer has to be predicted correctly and validation of CFD is critical.

## CFD VALIDATION FOR A STREET CANYON

Due to the complexity and scale of the built environment, CFD simulations are often conducted to predict the wind flow in urban areas (Moonen et al. 2012). To be able to rely on the CFD results, the simulations need to be validated by measurements. Nowadays RANS simulations with a k-ε turbulence model are still often applied for urban CFD simulations, due to its computational efficiency, although more advanced and more accurate CFD models exist (e.g. van Hooff and Blocken 2013, Kubilay et al. 2013). CFD models for flows in urban street canyons are not yet comprehensively validated in literature, especially for cases where buoyancy has an influence on the flow field. The aim the validation study is to conduct a more detailed validation for a wider range of different buoyant flow fields in urban street canyons.

### Experimental setup

Our own measurements (Allegrini et al. 2013) are used for validation purposes. To model the flow in an urban street canyon a cavity of W x H x L (W: width; H: height; L: length) 20 x 20 x 180 cm was constructed in the wind tunnel (Figure 1). The flow direction was perpendicular to the axis of the cavity. All surfaces of the wind tunnel model were made out of aluminium, which justifies not to model roughness in this validation study. The walls and the ground of the street canyon were heated individually with heating mats (mounted on the back of the aluminium plates). The flow field was measured with particle image velocimetry (PIV) on a cross-section (near the centre) of the street canyon. To characterise the flow in terms of buoyancy the Froude number was used in this study:

$$Fr = \frac{U_{FS}^2}{gH \frac{T_w - T_{ref}}{T_{ref}}} \quad (1)$$

Where  $U_{FS}$  is the freestream velocity,  $T_w$  is the surface temperature of the heated wall,  $T_{ref}$  is a reference temperature (here the temperature of the freestream) and  $g$  is the gravitational acceleration.

Table 1

Surface temperatures and Reynolds numbers with corresponding Froude numbers.

RE	70 °C	90 °C	110 °C	130 °C
9000	1.49	1.04	0.80	0.65
14200	3.68	2.58	1.99	1.62
19200	6.75	4.74	3.65	2.97
24600	11.11	7.79	6.00	4.88
30700	17.29	12.13	9.34	7.59

A wide range of Froude numbers was covered by testing at a wide range of surface temperatures and freestream velocities. The different boundary

conditions together with the respective Reynolds and Froude numbers are given in Table 1. The temperature at the inflow of the wind tunnel was for all cases 23 °C.

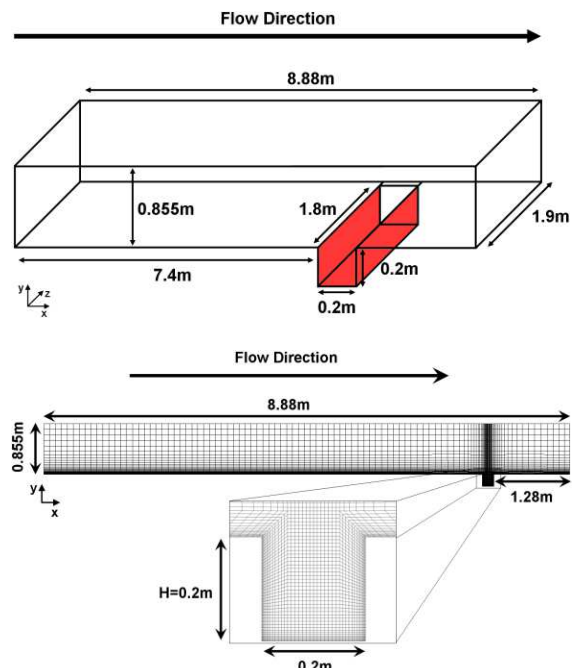


Figure 1: Dimensions of the wind tunnel model and computational domain.

### Numerical Model

For this validation study, 2D steady RANS CFD simulations using ANSYS Fluent 12.0 were conducted. The standard and the realizable k-ε models were used to model turbulence. At the near-wall regions the boundary layers were either resolved with low-Reynolds number modelling (LRNM) or modelled with wall functions (WFs). The dimensions of the 2D computational domain were set according to the wind tunnel dimensions (Figure 1). The mesh was built based on a grid sensitivity analysis and on guidelines of Franke et al. 2007. It was refined towards the walls and had maximum  $y^+$  values of 4.5. The same mesh was used for simulations with LRNM and for simulations with WFs, resulting in too low  $y^+$  values for simulations with WFs (the consequences of this selection are discussed in the following section). A mesh with high enough  $y^+$  values for WFs could not be used, because the mesh would be too coarse to resolve the global flow structures (width of first cell: >1 cm).

At the inlet the measured boundary layer profiles (Allegrini et al. 2013) for the velocity and the turbulent kinetic energy (TKE) were imposed. The incoming air temperature was 23 °C, to match the air temperature measured at the inlet of the test section. All surfaces were modelled without roughness, because no roughness can be defined with LRNM. This may be justified since the wind tunnel model was made out of aluminium with a very low surface

roughness. For the surfaces inside the street canyon, the surface temperatures obtained from the experiments were used as temperature boundary conditions. The surfaces outside the street canyon were modelled as adiabatic. Symmetry boundary conditions were imposed at the top boundary and outflow boundary conditions at the outlet.

To account for buoyancy the density, the specific heat capacity, the thermal conductivity and the viscosity were approximated with polynomial functions as a function of the temperature in the Navier-Stokes equations. Radiation was not considered directly in the CFD simulations, since constant temperature boundary conditions were imposed on the different street canyon surfaces.

## VALIDATION: RESULTS

### Approach flow

In order to achieve a good agreement between CFD and measured flow fields inside the street canyon, the approach flow in CFD has to match the measured approach flow profiles. In Figure 2 the approach flow profiles of the wind tunnel measurements and the CFD simulations at  $x = 7$  m are given for  $Re = 19200$  (standard  $k-\epsilon$  model; SWF: standard WF; NEWF: non-equilibrium WF). First simulations were conducted employing LRNM. There was a good agreement of the velocity profiles using LRNM compared with the measured data. The TKEs were however too low. The TKE was decaying in the streamwise direction in the CFD simulations. To avoid this decay, shear stresses at the surfaces up- and down-stream of the street canyon were predefined together with TKE sources in the flow up- and down-stream of the street canyon (dashed lines "LRNM source"). With this method the streamwise change of the approach flow profiles of the TKE can be decreased. The higher TKEs had however an impact on the velocity profiles. The velocities in the near-wall regions decreased and became too low, while in the freestream they were too high. Secondly, simulations were conducted using WFs. For the fine mesh in this study, the first grid points were in the viscous sublayer. In contrast to the LRNM, the damping of TKE in the viscous sublayer and the buffer layer cannot be captured. Due to this it is not recommended to use WFs for fine meshes. In this study WFs are nevertheless used, since the aim was to investigate if the results can be improved using WFs. Using the SWFs, the results for the velocity profiles deviated slightly more from measured values than for LRNM. The TKEs were slightly higher but still much lower compared to the measurements. As with LRNM, with source terms for the TKE the NEWFs underestimated the velocities in the near-wall regions and overestimated the velocities in the freestream. With NEWFs the peak of the TKE close to the ground can be captured, but the boundary layer was thicker than in the measurements.

Studying the approach flow profiles, it can be concluded that with the models employed in this study it is not possible to adjust both velocity and TKE profiles of the approach flow such that they match completely the measured profiles.

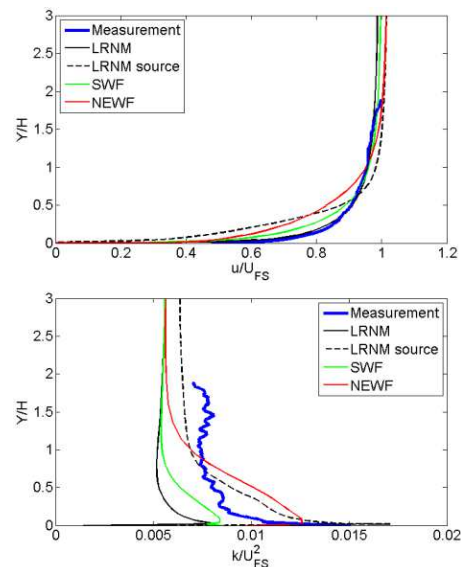


Figure 2: Normalised approach flow profiles of the velocity and TKE ( $Re = 19200$ ; standard  $k-\epsilon$  model).

### Isothermal case

For the isothermal cases the energy equation is not solved. In Figure 3 the normalized horizontal centreline profiles of the velocity and TKE are given for  $Re = 19200$ .

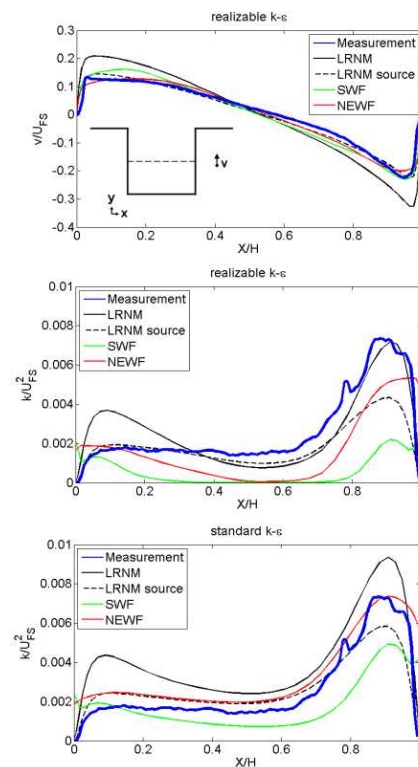


Figure 3: Normalised horizontal centreline profiles of the vertical velocity and TKE ( $Re = 19200$ ; standard and realizable  $k-\epsilon$  models).



The velocity profiles show that all models predict the vortex in the centre of the street canyon. LRNM overestimates the velocities close to the walls, while there is a good agreement for the simulations with WFs (and “LRNM source”). The standard  $k-\varepsilon$  predicts slightly higher TKEs inside the street canyon than the realizable  $k-\varepsilon$  model for LRNM. With the realizable  $k-\varepsilon$  model the TKEs are much too low in the centre of the street canyon using WFs. For WFs the results can be improved using a standard  $k-\varepsilon$  model. Best agreement can be found for the NEWFs with a standard  $k-\varepsilon$  model. Theoretically the LRNM should perform better. We think that LRNM shows less accurate results here, because of the decay in TKE in the approach flow (see below). In the following sections results of LRNM simulations with a standard  $k-\varepsilon$  model and NEWF simulations with a realizable  $k-\varepsilon$  model are presented.

### All surfaces heated

In this section cases with all three street canyon surfaces heated to the same temperature are studied, using Froude numbers of 6.75 and 17.29. These cases were chosen because CFD simulations and measurements show one main vortex in the centre of the street canyon, meaning that not only contour plots, but also centreline profiles can be compared. In Figure 10 normalised centreline profiles of the horizontal velocity and the TKE are given (up to  $0.75H$  above the street canyon). Besides the cases with LRNM and NEWF also simulations with NEWFs and a short upstream extension (only  $0.25H$ ) in front of the street canyon were conducted. With this short upstream domain (“NEWF short”), the boundary layer cannot develop and therefore the approach flow velocities do not decay as in the case with the long domain. In the boundary layer above the street canyon the simulation with NEWFs predicts velocities which are too low. With LRNM and “NEWF short” a very good agreement was found. In the shear layer at the top plane of the street canyon, the velocities are strongly decreased. At  $Y/H = 1$  the best agreement for the velocity can be observed for the NEWFs, while the other two models overestimate the velocities. Inside the street canyon the best agreement can be found for simulations using NEWFs, while to other two models overestimate the velocities close to the ground. Therefore it can be concluded that the velocities inside the street canyon are mainly influenced by the velocities in the shear layer. The near-wall treatment is less important and therefore LRNM and “NEWF short” show very similar results inside the street canyon. For the TKE all CFD models can capture the general trend. Thus it is important to correctly predict the flow in the approach flow as well as in the shear layer in order to get accurate results inside the street canyon.

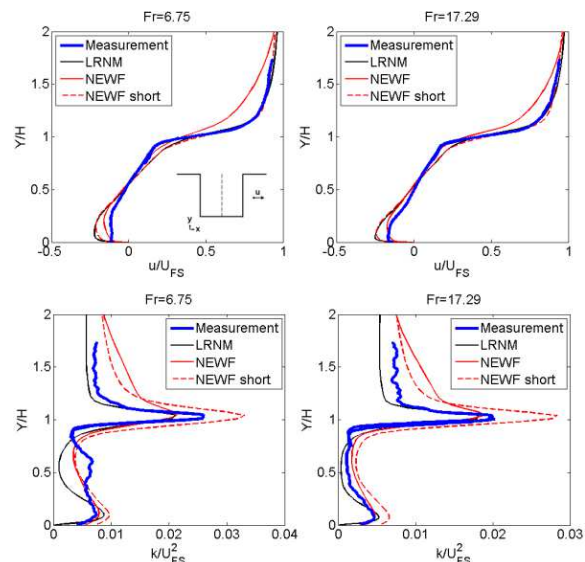


Figure 4: Normalized vertical centreline profiles of the horizontal velocity and TKE (LRNM with realizable  $k-\varepsilon$  model; NEWF with standard  $k-\varepsilon$  model).

## EVAPORATIVE COOLING IN A STREET CANYON

A first example of the urban microclimate model is the influence of evaporative cooling on the thermal comfort in a street canyon. The air flow due to forced convection and buoyancy, including heat and vapour transport in the air domain, is solved using CFD, the effect of solar and longwave radiation including multiple reflections is solved using a radiation model, while evaporative cooling in the porous urban materials is modelled using a heat and moisture transport model (Saneinejad et al. 2012). The 2D street canyon of  $10 \times 10$  m is exposed to two days during June taken from a typical meteorological year (TMY) of Zürich. The air temperature varies between  $13.5^\circ\text{C}$  and  $19^\circ\text{C}$  and the relative humidity varies between 62% and 86%. The windward wall is assumed to be wet after a rain shower ( $\text{RH} \approx 100\%$ ) while the other surfaces are dry. The walls of the canyon are made of ceramic brick (0.09 m thick) and have albedo of 0.4. The soil is covered with 0.1 m concrete layer, assumed to be dark colored with albedo of 0.1. The reference wind speed at 10 m height is 5 m/s.

To evaluate the effect of evaporative cooling, we compare the surface temperature at the top point (9.5 m), and bottom point (0.5 m) of the windward wall, as well as the average air temperature and relative humidity in the street canyon for two cases: (i) when the windward wall is initially wet, and (ii) when the windward wall is initially dry (Figures 5a-d). It can be seen that evaporative cooling results in a maximum drop of the wall surface temperature of  $15^\circ\text{C}$  at the top location (Figure 5) and  $13^\circ\text{C}$  at the bottom location (Figure 1) of the wall, during the first day of drying. The material at top and bottom is in its first drying phase, where water evaporates from

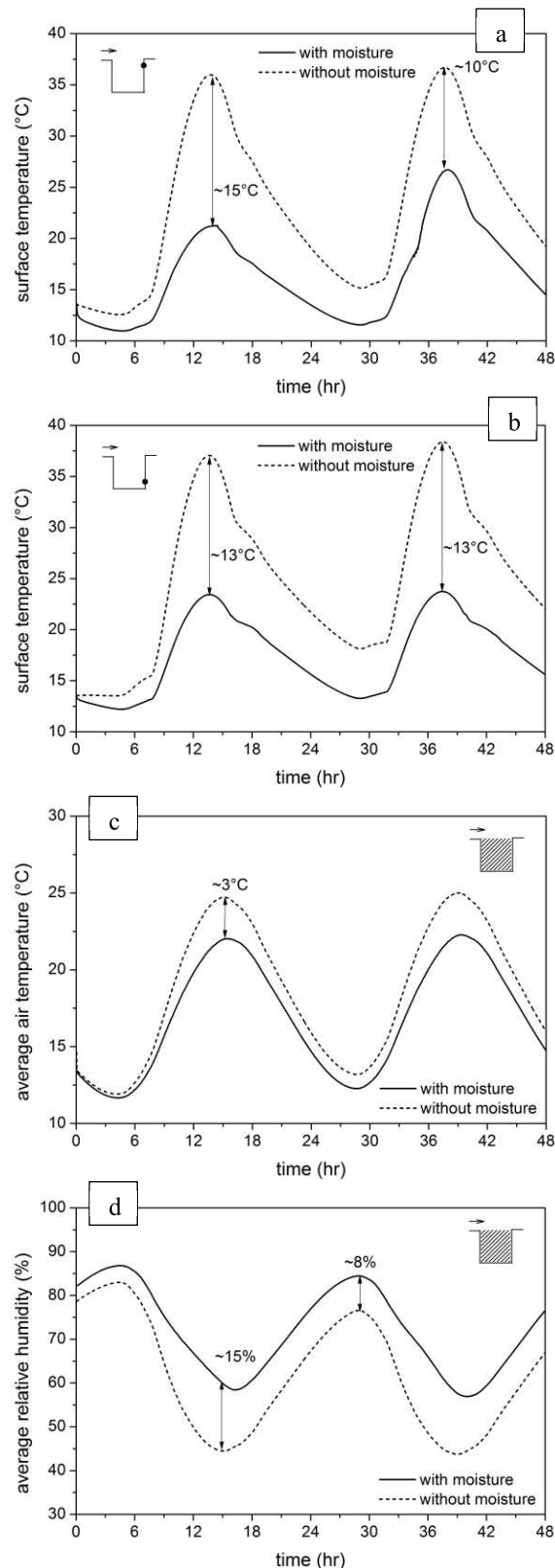


Figure 5. Comparison of cases with and without moisture (a) surface temperature at the height of 9.5 m, (b) surface temperature at the height of 0.5 m on the windward wall, (c) average air temperature and (d) average relative humidity in the street canyon

the surface of the wall, and a lot of latent heat is extracted. On the second day the temperature difference at the top location (Figure 5a) is less because the wall at this location has reached the second drying phase, where the moisture front recedes into the material and therefore less energy is required for evaporation. The average air temperature in the street canyon (Figure 5c) is approx. 3°C lower in the case with the wet wall, due to evaporative cooling. The average relative humidity (Figure 5d) is approx. 15% higher, compared to the dry case, due to mixing of moisture evaporated from the wall with the air in the canyon.

Further we evaluate the effectiveness of evaporative cooling by studying the comfort conditions of a person standing in the street canyon. For this study, a 1.8 m tall person standing 1 m away from the windward wall is considered. To study the comfort of this person, we use the universal thermal climate index (UTCI) (Fiala et al, 2012). The parameters used for determining the UTCI are the air temperature, the vapor pressure, the wind speed and the mean radiant temperature.

Figure 6a shows the UTCI for a person standing 1 m away from the windward wall, for two cases, i.e. with and without evaporative cooling. It can be seen that the person can feel up to max. 2.5°C cooler during the warmest part of the day on the first day and 2.7°C on the second day due to evaporative cooling. To understand this phenomena better, we look at the four parameters which influence the UTCI at the studied location, being the air temperature, the mean radiant temperature ( $T_{mrt}$ ), the vapour pressure or RH), and the wind speed. The evolution of these parameters during the 48 hr of drying, for cases with and without moisture, is shown in Figures 2b, c, d, e and f. It can be seen that for the case with moisture, the air temperature and  $T_{mrt}$  at the studied location are approx. 2°C and 8°C lower in comparison to the case without moisture, respectively, while the vapor pressure is approx. 2 hPa (relative humidity approx. 15%) higher and the wind speed is approx. 0.3 m/s lower. Lower air temperature and radiant temperature due to evaporative cooling result in an improved thermal comfort, while a higher relative humidity and lower wind speed result in a lower thermal comfort. The more comfortable conditions during the second day is that some parts of the wall are already in the (second drying phase and dry slower, resulting in a lower vapor pressure in the street canyon.

Further a parametric study shows that the evaporative cooling is most effective when the wind speed is low, since in this case the removal of heat by wind is less efficient.

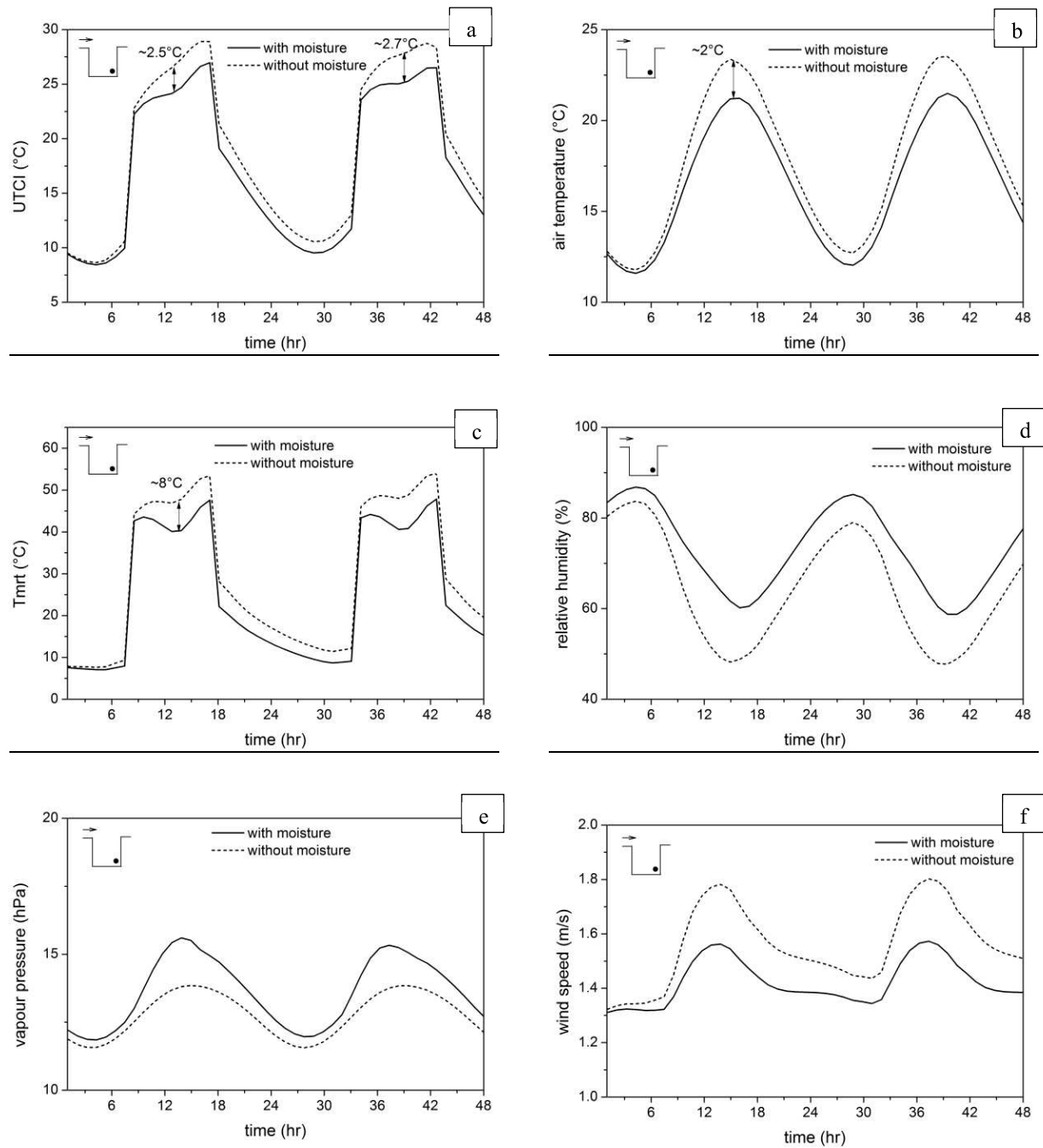


Figure 6. Comparison of cases with and without moisture for a) UTCI b) air temperature c) mean radiant temperature d) relative humidity e) vapour pressure and f) wind speed, at the position of a person standing 1 m from the windward wall.

## SPACE COOLING DEMANDS IN STREET CANONS: MODELLING

In a second example, the impact of the urban microclimate on the space heating and cooling energy demand of buildings is demonstrated and quantified for typical office buildings in street canyon configurations (Allegrini et al., 2012a). Street canyons are chosen as a generic urban configuration. For this study, the transient 3D single building multi-

zone BES software *TRNSYS 17.0* (TRNSYS 17.0, 2010) is employed and adapted to account for the following three aspects of urban microclimate: (i) the radiation exchange between neighbouring buildings, (ii) the convective heat transfer adapted to the local flow field, and (iii) the UHI effect.

### Radiation exchange

In classical BES of stand-alone buildings, solar irradiation on façades is considered as a gain and long-wave radiation as a heat loss to the cold sky. In street canyon configurations, however, the solar and long-wave radiation fluxes are characterized by multiple diffuse and specular reflections at the building surfaces. In *TRNSYS 17*, the 3D radiation

model that accounts for these reflections normally is only used for interior zones. Therefore, in this study, the outdoor space between buildings is modelled as an atrium with an open ceiling. In this way, the shadowing by the neighbouring buildings and the exchange of long-wave and solar radiation between the different buildings is considered. The exchange of solar diffuse and long-wave radiation is determined using Gebhart factors, which basically are view factors, corrected to include the effect of multiple reflections.

### Convective heat transfer

The convective heat transfer at the building envelope is modelled using convective heat transfer coefficients (CHTCs). Usually the CHTCs are based on measurements at façades of stand-alone buildings. For BES of buildings in urban areas CHTCs derived for stand-alone buildings can lead to inaccurate convective heat transfer predictions. To consider the reduced convective heat transfer at the building façades, computational fluid dynamic (CFD) simulations were conducted, for which specific temperature wall functions were derived (Allegrini et al., 2012b). Then CHTC vs. reference wind speed correlations were derived for different stand-alone and urban building configurations and used in BES for the specific urban geometries considered. These CFD simulations were also validated by wind tunnel measurements (see below). Figure 7 gives examples of CHTC correlations for different building configurations.

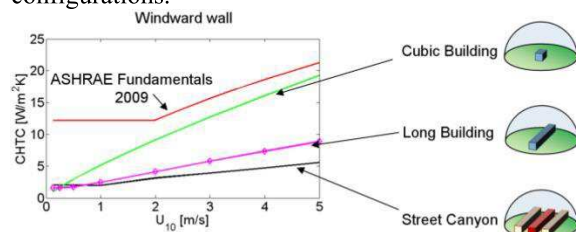


Figure 7. CHTC vs. wind speed at the windward wall for different building configurations

### Urban heat island intensity

The climatic data for the Swiss city of Basel are used as input for the BES. An UHI intensity approximation was developed based on measured data of the BUBBLE project (Rotach et al., 2005).

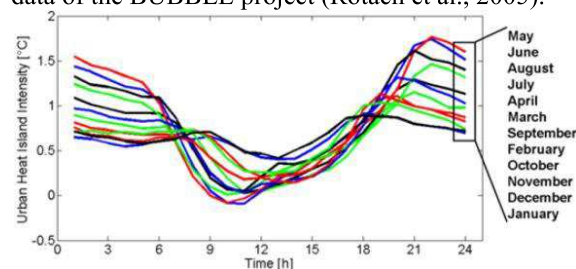


Figure 8. Average diurnal UHI intensity schedules for each month of a year

A diurnal schedule of the temperature difference between the rural (here Basel-Binningen) and the urban (here Basel-Spalenring) air temperature was

specified for each month. For each hour of the day, the temperature differences are averaged for a time period of 7 years. The profiles are given in figure 8. For the BES, these hourly intensity values are then added to the basic weather file of the rural station.

### Buildings

In this study, three-storey buildings with different surroundings are analysed. BESs are performed for stand-alone buildings in an open field and for the same buildings with street canyons in front and behind the buildings. Street canyons with aspect ratios of 0.5, 1 and 2 are considered (aspect ratio  $H/W$  with  $H$ : height of the building,  $W$ : street canyon width). Figure 9 depicts the studied building surrounded by street canyons with aspect ratios of one. The studied building has a length of 110.5m (to minimize lateral boundary effects in the radiation model) and a total height and width of 13.5m.

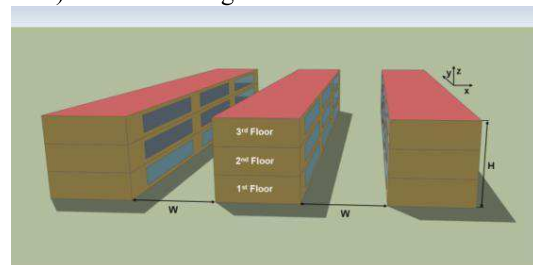


Figure 9. The building of interest in the middle, surrounded by street canyons with aspect ratios of 1 ( $H/W$ )

The building is well insulated externally with a  $U$ -value for the walls of  $0.26\text{W/m}^2\text{K}$ , roof of  $0.15\text{W/m}^2\text{K}$  and ground floor of  $0.30\text{W/m}^2\text{K}$  (no basement considered). The glazing fraction is 50% and windows with double-glazing ( $U$ -value  $1.4\text{W/m}^2\text{K}$ ,  $g$ -value 0.589) are assumed. Internal gains by lights, devices and persons and occupancies are set according to (SIA 2024, 2006) (standard values for offices are used). Light control is as follows: lights are on when the building is occupied and the solar radiation on the corresponding façades is  $<70\text{W/m}^2$ . External shading devices are closed when solar radiation on the corresponding façades is  $>120\text{W/m}^2$ . The building has an orientation showing a north and south façade, lateral façades are modelled as adiabatic. A mechanical ventilation system is used (Day-time: airflow rate  $30\text{m}^3/\text{h}$  per person, heat recovery with 80% efficiency, ambient air is not heated to temperatures above  $21^\circ\text{C}$ ; Night-time: air change of  $1\text{h}^{-1}$  if building needs to be cooled). Space cooling and space heating demands were determined for room air temperatures controlled to remain between  $21^\circ\text{C}$  and  $26^\circ\text{C}$  by heating or cooling. The change in for e.g. electricity demand due to changed artificial lighting demands, caused by shadowing, is not considered.

The street canyon building studied is surrounded by two other rows of buildings, which have the same properties as the studied building. The energy demands of these two buildings are not evaluated.



## SPACE COOLING DEMANDS IN STREET CANONS: RESULTS

### Annual space cooling demands

Figure 10 shows the annual space cooling demands for a stand-alone building and a building surrounded by street canyons with different aspect ratios. In modelling case 1 (“radiation effects”), the same CHTC correlations are used for the stand-alone as well as for the street canyon configurations, namely CHTC correlations that were derived for stand-alone buildings. In case 2 (“+dynamic CHTC”), CHTC correlations derived by CFD (Allegrini et al., 2012b) are used for the street canyon. Case 3 (“+heat island effect”) is identical to case 2, but with the UHI intensities considered. The space cooling demand for the stand-alone buildings is much lower compared to the buildings situated in the street canyons. For wider street canyons, the cooling demand is higher, because more solar and thermal radiation is entrapped, mainly due to multiple reflections. In narrow street canyons, the cooling demand is lower due to less solar radiation entering the street canyon. The different CHTC correlations become only important for narrow street canyons. The UHI effect significantly increases the space cooling demand for all cases. The differences in space cooling demands between standalone and street canyon buildings are rather high due to the fact that the space cooling demands for the former are very low (for the climate of Basel). Therefore, already moderate changes of the absolute values cause rather high relative differences. For the space heating demand the differences between the different cases are much lower than for the cooling. In general, higher surface and air temperatures cause a decrease of the heating demands.

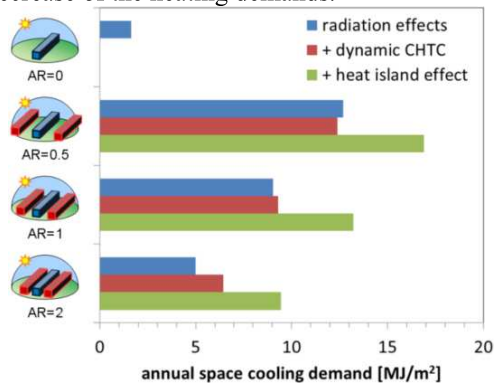


Figure 10. Annual space cooling demands for different modelling cases and street aspect ratios

## CONCLUSIONS

An urban microclimate model is presented, which consists of an air flow model solved by CFD, a heat and moisture transport model taking into account evaporative cooling effects by porous urban surfaces, a radiation model taking into account solar and longwave radiation including multiple reflections and a building energy simulation model. In this paper we present validation study with wind tunnel results. The

results show that CFD can predict the general flow structures and the influence of buoyancy. The detailed flow field inside the street canyon is strongly dependent on the flow structure inside the shear layer at the top of the street canyon. Therefore to get accurate results for the flow profiles inside the street canyon, the flow inside the shear layer has to be predicted correctly. Then, the urban microclimate model is used to study the effect of evaporative cooling on thermal comfort in a street canyon. It is shown that evaporative cooling can enhance the thermal comfort at low wind speeds by cooling down the urban surfaces and the air in the street canyon. However, due to the evaporation the relative humidity of the air in the street canyon increases, which results in a lowering of the thermal comfort. In a second part of this paper we show that for buildings in an urban setting (compared to stand-alone buildings) the urban microclimate can have a significant impact on the heat exchange and thus on the energy demand of buildings, depending on building geometries and constructions. In the street canyon case presented, solar and long-wave radiation effects had the greatest impact, followed by the UHI effects and the convective heat exchange both at the surfaces and in the canyon to free-stream shear layer.

## REFERENCES

- Allegrini J., Dorer V., Carmeliet J. 2012a. Influence of the urban microclimate in street canyons on the energy demand for space cooling and heating of buildings. *Energy and Buildings* 55, 823-832
- Allegrini J., Dorer V., Defraeye T., Carmeliet J. 2012b. An adaptive temperature wall function for mixed convective flows at exterior surfaces of buildings in street canyons. *Building and Environment* 49, 55-66
- Allegrini J., Dorer V., Carmeliet J. 2013. Wind tunnel measurements of buoyant flows in street canyons. *Building and Environment* 59, 315-326
- Fiala D, Havenith G, Bröde P, Kampmann B, Jendritzky G. 2012. UTCI-Fiala multi-node model of human heat transfer and temperature regulation. *Int J Biometeorol.* 56(3):429-41.
- Franke, J., Hellsten, A., Schlünzen H., Carissimo, B., 2007. Best practice guideline for the CFD simulations of flows in the urban environment. COST Action.
- Kubilay, A., Derome, D., Blocken, B., and Carmeliet, J., 2013. CFD simulation and validation of wind-driven rain on a building façade with an Eulerian multiphase model. *Building and Environment* 61, 69-81.
- Moonen, P., Defraeye, T., Dorer, V., Blocken, B., and Carmeliet, J., 2012. Urban physics: Effect of the microclimate on comfort, health and energy demand. *Frontiers of Architectural Research*, 1 (3), 197-228.
- Rotach M.W. et al. 2005. BUBBLE – an Urban Boundary Layer Meteorology Project. *Theor. and Appl. Climat.* 81, 231- 261
- Saneinejad S, Moonen P, Defraeye T, Derome D, Carmeliet J: Coupled CFD, radiation and porous media transport model for evaluating evaporative cooling in an urban environment. *Journal of Wind Engineering & Industrial Aerodynamics* 104-106: 455–463, 2012.
- SIA 2024. 2006. Guidelines for standard internal loads for energy and building services engineering. Swiss Society of Engineers and Architects (SIA), Zürich
- TRNSYS 17.0. 2010. Transient System Simulation Program. SEL, University of Wisconsin/ TRANSSOLAR, Stuttgart
- Van Hooff, T., and Blocken B., 2013. CFD evaluation of natural ventilation of indoor environment by the concentration decay method: CO<sub>2</sub> gas dispersion from a semi-enclosed stadium. *Building and Environment* 61, 1-17.